Enantioselective Synthesis of β-Blockers *via* Hydrolytic Kinetic Resolution of Terminal Oxiranes by Using Bimetallic Chiral {{2,2′-[Cyclohexane-1,2-diylbis(nitrilomethylidyne)]bis[phenolato]}(2−)}cobalt ([Co(salen)])-Type Complexes

by **Rahul B. Kawthekar** and **Geon-Joong Kim***

Department of Chemical Engineering, Inha University, Incheon, South Korea, 402751
(phone: +82-32-860-7472; fax: +82-32-872-0975; e-mail: kimgj@inha.ac.kr)

The synthesis of chirally pure β-blockers was successfully achieved *via* hydrolytic kinetic resolution of butyl (±)-4-(oxiran-2-ylmethoxy)benzeneacetate ((±)-**1**) and (±)-4-(oxiran-2-ylmethoxy)benzeneacetonitrile ((±)-**2**) in the presence of bimetallic chiral [Co(salen)]-type complexes. The newly synthesized bimetallic chiral [Co(salen)]-type complexes exhibited excellent enantioselectivities of up to >98% ee in good yields (*Tables 1–3*).

Introduction. – The synthesis of chirally pure β-blockers is a very important task in the asymmetric catalysis as well as of pharmaceutical interests [1]. The β-adrenergic blocking agents (β-blockers) are used as antihypertensive drugs, they reduce the risk of producing long-lasting cardiac depression, since the effect of the drug would rapidly dissipate upon termination of the infusion [2]. In this category, atenolol (=4-{2-hydroxy-3-[(1-methylethyl)amino]propoxy}benzeneacetamide) and propranolol (=1-[(1-methylethyl)amino]-3-(naphthalen-1-yloxy)propan-2-ol) are the most important and widely prescribed drugs on the large scale [3]. In the last 15 years, numerous efforts have been devoted to the synthesis of β-blockers *via* lipase catalysis or hydrolytic kinetic resolution (HKR), or by a nitrile hydration catalytic method [4]. To the best of our knowledge, only a few syntheses of atenolol from racemic epichlorohydrine (=2-(chloromethyl)oxirane; ECH) have been reported [5]. On the basis of these facts, the great utility of chiral oxiranes in stereoselective synthesis provided the motivation to develop a new method from which chiral atenolol could be prepared from racemic oxiranes. Among these available methods, HKR provides a general protocol to achieve highly enantiomer-enriched chiral building blocks that are available from inexpensive racemic materials [6]. In our previous study, we have shown that [Co(salen)]-type complexes bearing group-13 transition-metal salts display good enantioselectivity and reactivity for the HKR of racemic terminal oxiranes [7].

In continuation of our efforts directed towards the designing of bimetallic chiral [Co(salen)]-type catalyst systems for HKR, we report herein a new method to produce bimetallic chiral [Co(salen)]-type catalysts bearing transition-metal salts attached to the O-atoms of the salen-type complexes, and their successful application to the HKR of various terminal epoxides. This type of salen catalysts has never been used as a

catalyst in enantioselective asymmetric catalysis and is now shown to be remarkably efficient and highly enantioselective in HKR reactions.

Results and Discussion. – We screened a series of chiral [Co(salen)]-type complexes (*Fig. 1*) containing various transition-metal salts to evaluate the most reactive and enantioselective catalyst in the HKR of (±)-2-(phenoxymethyl)oxirane by using 0.55 equiv. of H_2O as a nucleophile (*Table 1*). The catalysts **a**, **e**, **f**, and **h** (*Table 1*, *Entries 2*, *14*, *17*, and *23*) exhibited superior enantioselectivities to those of the catalysts **b**, **c**, **d**, and **g** (*Entries 5*, *8*, *11*, and *20*). The reactions proceeded smoothly with 0.3 mol-% of one of the catalysts **a**–**h** under solvent-free conditions at room temperature, affording the recovered chiral oxirane in good yield with mostly high ee (*Table 1*). The amount of catalyst was varied from 0.05 to 0.3 and 1.0 mol-% to investigate its effect on the enantioselectivity in the HKR of 2-(phenoxymethyl)oxirane. The enantioselectivity of the product was measured periodically at room temperature, establishing that it increased rapidly at 0.3 mol-% of catalyst to 99% ee in the case of **a**. Also at 0.05 mol-% of catalyst, a high ee value (98%) was achieved when the reaction was prolonged. However, with the increase of the catalyst amount to 1.0 mol-%, no significant effect was observed on the enantioselectivity, and no decrease of the reaction time occurred. Therefore, we decided to use 0.5 mol-% of catalyst for further experiments.

Fig. 2 shows the activities of the catalysts **a**–**h** in the asymmetric resolution of butyl (±)-4-(oxiran-2-ylmethoxy)benzeneacetate ((±)-**1**) in the presence of 0.5 mol-% of

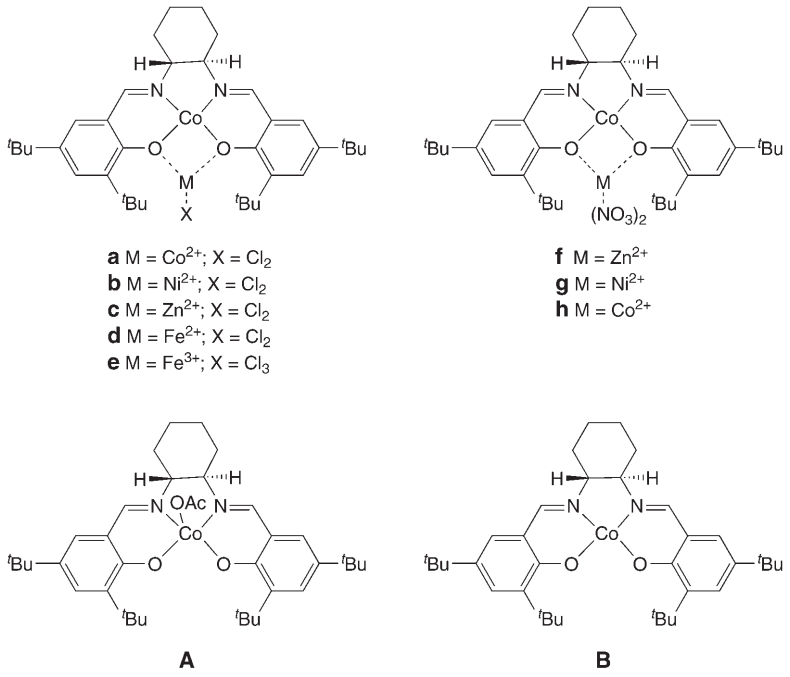

Fig. 1. *Bimetallic chiral [Co(Salen)]-type complexes* **a**–**h** *and reference complexes* **A** *and* **B**

Table 1. *Optimization of Chiral [Co(Salen)]-Type Complexes in HKR of (±)-2-(Phenoxymethyl)oxirane*

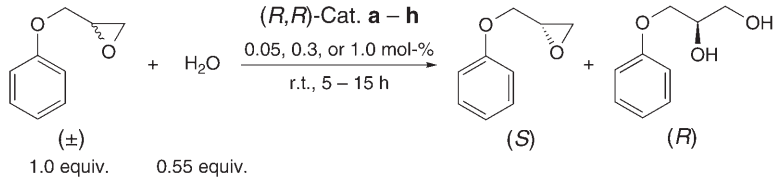

(±) 1.0 equiv. 0.55 equiv. (*S*) (*R*)

Entry	Catalyst	mol-% [a])	Yield [%] [b])	ee [%] [c])
1	**a**	0.05	45	98
2	**a**	0.3	45	99
3	**a**	1.0	45	99
4	**b**	0.05	40	70
5	**b**	0.3	40	70
6	**b**	1.0	40	70
7	**c**	0.05	39	88
8	**c**	0.3	43	84
9	**c**	1.0	43	84
10	**d**	0.05	42	85
11	**d**	0.3	40	86
12	**d**	1.0	40	86
13	**e**	0.05	40	98
14	**e**	0.3	40	98
15	**e**	1.0	40	98
16	**f**	0.05	40	98
17	**f**	0.3	40	98
18	**f**	1.0	40	98
19	**g**	0.05	40	85
20	**g**	0.3	42	86
21	**g**	1.0	42	86
22	**h**	0.05	40	96
23	**h**	0.3	40	95
24	**h**	1.0	40	95

[a]) Catalyst loading on a per Co basis relative to racemic oxirane. [b]) Yield of isolated oxirane. [c]) Determined by HPLC or GC.

catalyst. The HKR of (±)-**1** with catalyst **a**, **e**, **f**, or **h** was particularly efficient in terms of both enantioselectivity (ee 93–98%) and fast reaction rate (*Table 2*, *Entries 9–12*). The application of the HKR method to (±)-**1** resulting in a *ca.* 40% yield of one enantiomer enables to envisage a straightforward strategy for the synthesis of β-blockers, since this enantiomer represents an interesting building block for the elaboration of a variety of chiral intermediates (see below).

The above-described HKR method was also applicable to a series of other terminal-oxirane derivatives. In particular, the oxiranes containing a *Lewis*-base functionality such as a CN group were established to be the best substrate with regard to enantioselectivity. The kinetic resolutions of (±)-4-(oxiran-2-ylmethoxy)benzeneacetonitrile ((±)-**2**) in the presence of 0.5 mol-% of catalyst **a** or **e** was complete and led to highly enantiomer-enriched (*S*)-**2** in *ca.* 40% yield (*Table 2*, *Entries 4* and *5*). This

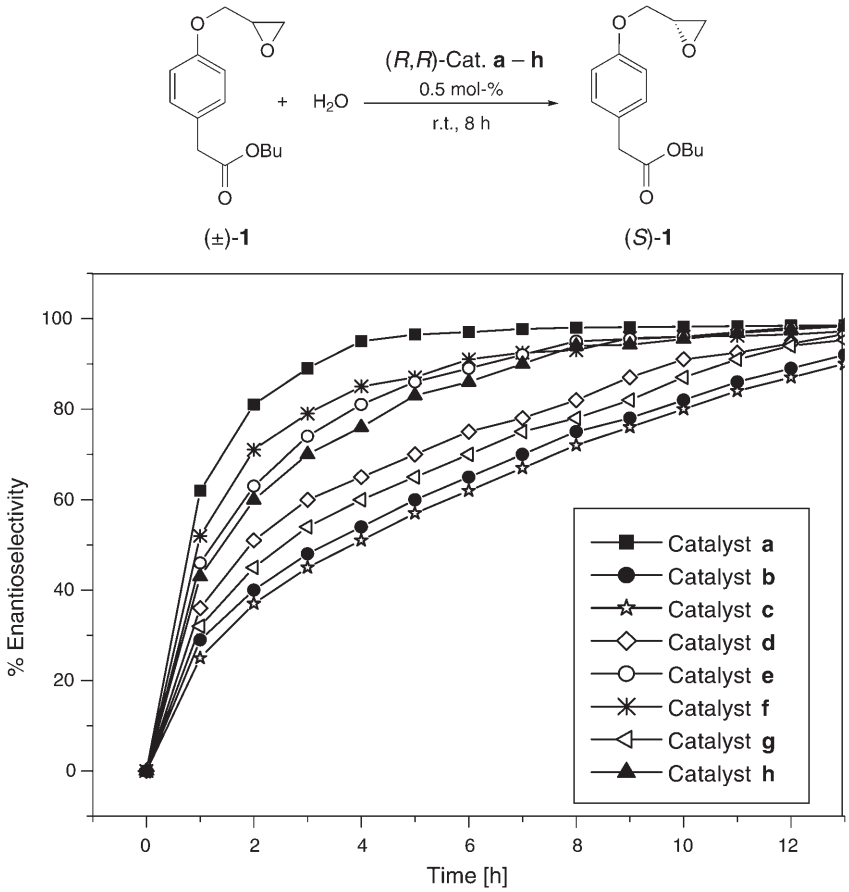

Fig. 2. *The catalytic activities of chiral [Co(Salen)]-type complexes* **a**–**h** *in the asymmetric HKR of butyl (±)-4-(oxiran-2-ylmethoxy)benzeneacetate* ((±)-**1**) *in the presence of 0.5 mol-% catalyst at room temperature*

reaction is noteworthy because of the easy synthetic procedure and the functional versatility of the optically active product (*S*)-**2**. As can be seen from *Fig. 3*, the enantiomer purity of the product was reached to 90–94% ee by decreasing the loading amount of catalyst to 0.05 mol-%, requiring longer reaction time to attain the high ee value in HKR, but the racemic oxirane derivatives were neverthless resolved successfully (*Table 2*, *Entries 1–3*). The reaction with the mononuclear catalyst such as the *Jacobsen*-type catalyst **A** (*Fig. 1*) at the 0.05 mol-% level did not lead to measurable conversion. By the mononuclear catalyst, the second-order dependence on concentration was found through intermolecular monometallic pathway. The enantioselectivity displayed by catalysts **a**, **e**, and **f** was independent on the catalyst loading, indicating that a highly selective intramolecular, cooperative process dominates within one salen unit [8].

Table 2. *Hydrolytic Kinetic Resolution of Various Terminal Oxirane Derivatives in the Presence of [Co(salen)]-Type Complexes*

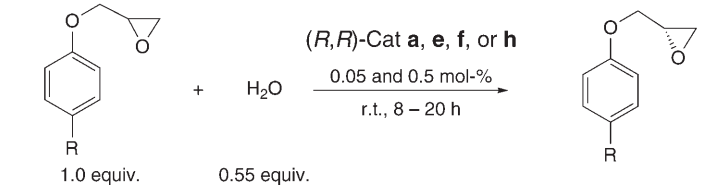

(±)-**1** R = CH_2COOBu
(±)-**2** R = CH_2CN
(±)-**3** R = CH_2COOEt
(±)-**4** R = CH_2COOMe

(*S*)-**1** R = CH_2COOBu
(*S*)-**2** R = CH_2CN
(*S*)-**3** R = CH_2COOEt
(*S*)-**4** R = CH_2COOMe

Entry	R	Catalyst	mol-% [a])	Yield [%] [b])	ee [%] [c])
1	CH_2CN	**a**	0.05	39	95
2	CH_2CN	**e**	0.05	39	93
3	CH_2CN	**f**	0.05	39	90
4	CH_2CN	**a**	0.5	40	98
5	CH_2CN	**e**	0.5	40	97
6	CH_2CN	**f**	0.5	40	94
7	CH_2CN	**h**	0.5	36	96
8	CH_2COOBu	**a**	0.05	35	98
9	CH_2COOBu	**a**	0.5	40	98
10	CH_2COOBu	**e**	0.5	40	95
11	CH_2COOBu	**f**	0.5	38	93
12	CH_2COOBu	**h**	0.5	39	94
13	CH_2COOEt	**a**	0.5	39	95
14	CH_2COOEt	**e**	0.5	39	94
15	CH_2COOEt	**f**	0.5	38	94
16	CH_2COOEt	**h**	0.5	38	93
17	CH_2COOMe	**a**	0.5	32	92
18	CH_2COOMe	**e**	0.5	31	92
19	CH_2COOMe	**f**	0.5	30	90
20	CH_2COOMe	**h**	0.5	30	90

[a]) Catalyst loading on a per Co basis relative to racemic oxirane. [b]) Yield of isolated oxirane. [c]) Determined by HPLC or GC.

Oxiranes containing an ester functionality other than that of (±)-**1** were also examined as substrates for the HKR. The kinetic resolution of ethyl (±)-4-(oxiran-2-ylmethoxy)benzeneacetate ((±)-**3**; *Table 2*, *Entries 13–16*) were effected in a straightforward manner in the presence of 0.5 mol-% of **a**, **e**, **f**, or **h** with 93–95% ee in 38–40% yield. The HKR of methyl (±)-4-(oxiran-2-ylmethoxy)benzeneacetate ((±)-**4**; *Table 2*, *Entries 17–20*) was also performed under similar conditions, but a somewhat lower enantioselectivity (ee 90–92%) was observed in these cases. The synthesis of (*S*)-atenolol (**6**) by using the HKR method is outlined in *Scheme 1*. The kinetic resolution of the butyl ester (±)-**1** was achieved in a highly efficient manner, providing the synthetically important (*S*)-oxirane intermediate (*S*)-**1** with high optical purity in

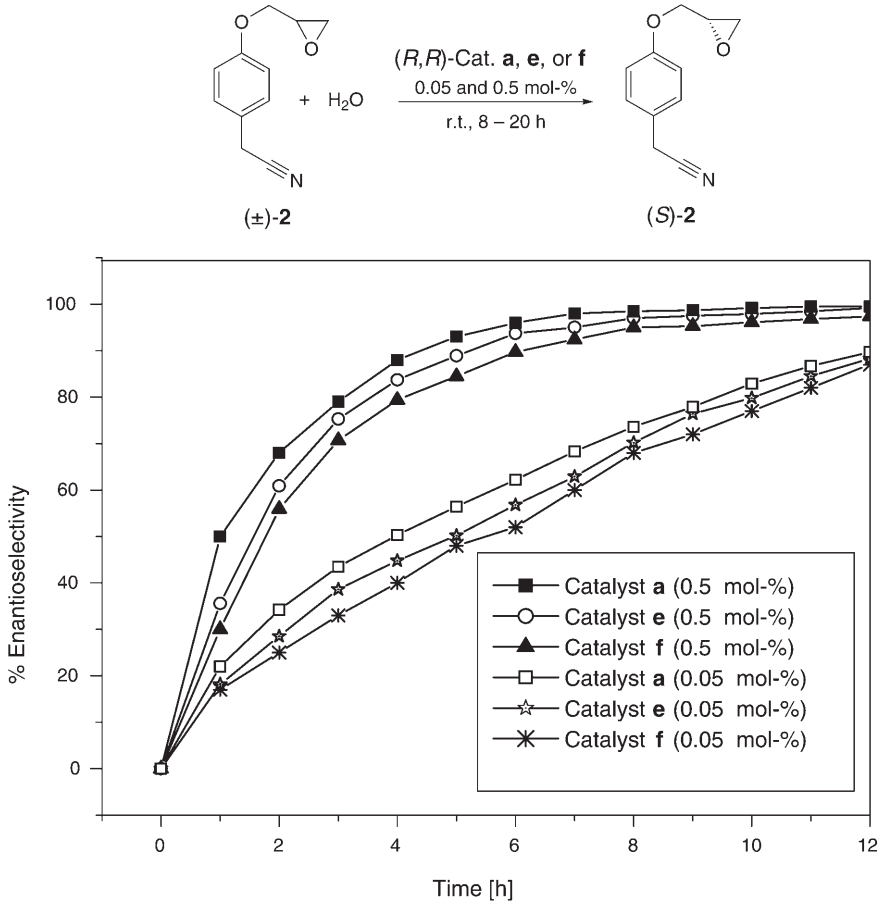

Fig. 3. *The effect of the loading amount of catalyst* **a**, **e**, *and* **f** *on the enantioselectivity of (±)-4-(oxiran-2-ylmethoxy)benzeneacetonitrile* ((±)-**2**) *in the presence of 0.05 and 0.5 mol-% of catalyst at room temperature*

excellent yield. Further transformation into (*S*)-atenolol (**6**) was accomplished by well-known methods, *i.e.*, by addition of excess $^{i}PrNH_2$ in presence of H_2O at reflux temperature (**5**), followed by treatment with aqueous NH_4OH. This straightforward transformation is a useful alternative to existing methods.

To explore the utility of chiral Co complexes for further enantioselective ring opening of terminal-oxirane derivatives, (±)-2-[(naphthalen-1-yloxy)methyl]oxirane ((±)-**7**) was evaluated as a substrate for the HKR (*Scheme 2* and *Table 3*). The HKR of (±)-**7** in the presence of catalyst **a** was very efficient and highly enantioselective. By using only 0.5 mol-% of catalyst, the resolution proceeded to completion within 8 h, forming the (*S*)-oxirane with excellent ee. This chiral oxirane was then treated with the $^{i}PrNH_2$ to provide an enantiomer-enriched propranolol (*Scheme 2*).

Scheme 1. *Synthesis of* (–)-(S)*-Atenolol* (**6**) *by Using Bimetallic Chiral [Co(Salen)]-Type Complex* **a**

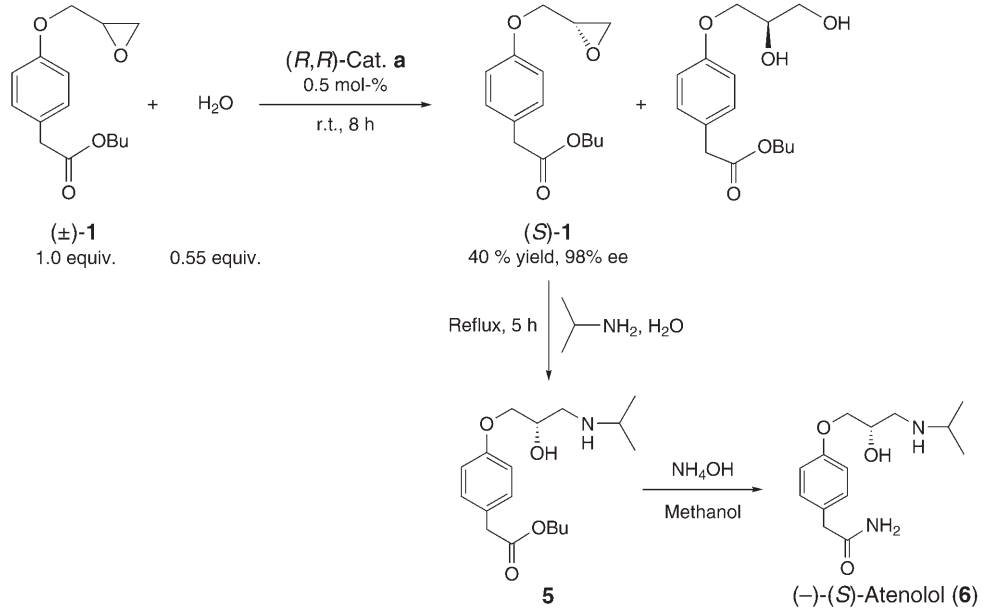

Scheme 2. *Synthesis of (S)-Propranolol* (**8**) *by Using Bimetallic Chiral [Co(Salen)]-Type Complex* **a**

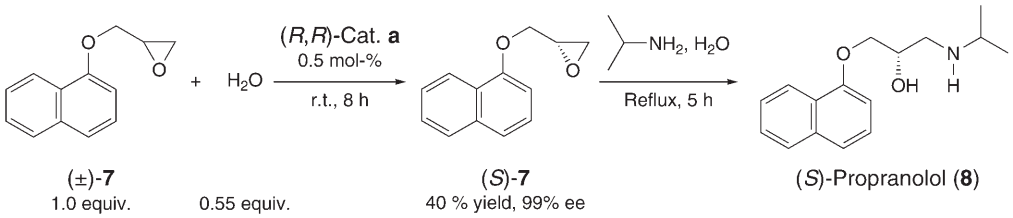

Summarizing, the HKR of terminal oxiranes was established as an efficient, synthetically useful enantiomer-separation method applicable to a broad range of substrates and suggesting a great potential of this strategy for product generation on an industrial scale, as shown in *Scheme 3*.

The chiral [Co(salen)]-type complexes were characterized by EXAFS and ESCA analysis. ESCA (electron spectroscopy for chemical analysis) was used to analyze and identify the environment created by the attachment of a transition-metal to the salen-type complex. ESCA Spectra can also provide useful information about the element's oxidation state. The chemical environment of an atom affects the strength with which electrons are bound to it. Atoms in different chemical environments produce peaks of slightly different binding energies. The results of ESCA analysis for the newly synthesized salen-type catalysts are given in *Table 4* and *Fig. 4*, and compared with the Co^{III}–OAc *Jacobsen*-type catalyst **A** and the [Co^{II}(salen)]-type complex **B** as reference

Table 3. *Hydrolytic Kinetic Resolution of (±)-2-[(Naphthalen-1-yloxy)methyl]oxirane* ((±)-**5**) *in the Presence of Chiral [Co(salen)]-Type Complexes*

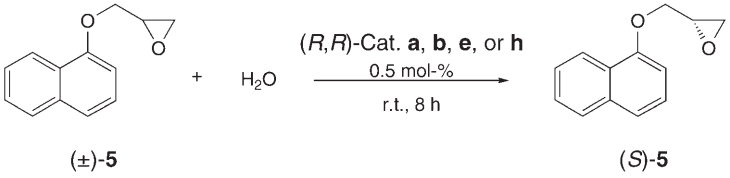

Entry	Catalyst	mol-% [a])	Yield [%] [b])	ee [%] [c])
1	**a**	0.5	40	99
2	**b**	0.5	32	70
3	**e**	0.5	39	95
4	**h**	0.5	35	92

[a]) Catalyst loading on a per Co basis relative to racemic oxirane. [b]) Yield of isolated oxirane. [c]) Determined by HPLC or GC.

samples. For complex **A**, the Co2p3 spectrum shows the peak at *ca.* 780 eV, which is attributed to the Co^{3+} ion [9][10]. *Jacobsen*-type catalyst **A** contains an AcO^- anion and is obtained on oxidation of the [Co^{II}(salen)]-type complex **B** with AcOH under air, it is clear that the binding energy of cobalt (Co2p3) was shifted from a higher to a lower value due to the change of the oxidation state from II to III [11]. Comparing the ESCA spectra of $Co^{II}-NiCl_2$ complex **b** and $Co^{II}-Co(NO_3)_2$ complex **h** with the spectrum of **B** established that the peaks for their Co2p3 at 781 eV arose from Co^{2+} ions, the corresponding values being identical to that of **B**, which was used as a starting compound. This result means that the Co^{II} oxidation state was retained during the formation of the transition-metal-salt-containing complexes **b** and **h** from **B**.

The binding energy of O1s (O-atom of the salen-type ligand) of the *Jacobsen*-type catalyst **A** and the [Co^{II}(salen)]-type catalyst **B** were found at *ca.* 531 eV, whereas those of $Co^{II}-NiCl_2$ complex **b** and $Co^{II}-Co(NO_3)_2$ complex **h** were shifted towards a higher value, *i.e.*, to 532.5 eV, respectively (*Fig. 4* and *Table 4*). In the case of **A**, the AcO^- anion is present to balance the positive charge of the Co-center, which is +3; but there is no interaction between such an anion and the O-atom of the salen-type ligand. Therefore, the binding energies of O1s did not vary between **A** and **B**. Thus, the change in binding energy of O1s of the salen-type ligand of **b** and **h** is generated by the anchoring of the transition-metal species to the ligand O-atoms by a *Lewis*-acid interaction.

EXAFS (Extended X-ray absorption fine structure) analysis can be used to determine the coordination number and bond length in the salen-type ligand; corresponding data for the newly synthesized chiral [Co(salen)]-type complexes are shown in *Table 5*. *Fourier*-transformed X-ray structure data were obtained experimentally and compared to the results obtained by the FEFF 6 program to calculate the coordination number and bond length, *etc.* To analyze the details of the measured spectra, curve fitting of the EXAFS spectra with the theoretically calculated spectra was carried out with FEFF 6 [12] (*Fig. 5*).

Scheme 3. *Schematic Representation of the HKR Reactions Leading to Atenolol and Propranolol by Using the Bimetallic Chiral [Co(Salen)]-Type Complex* **a**

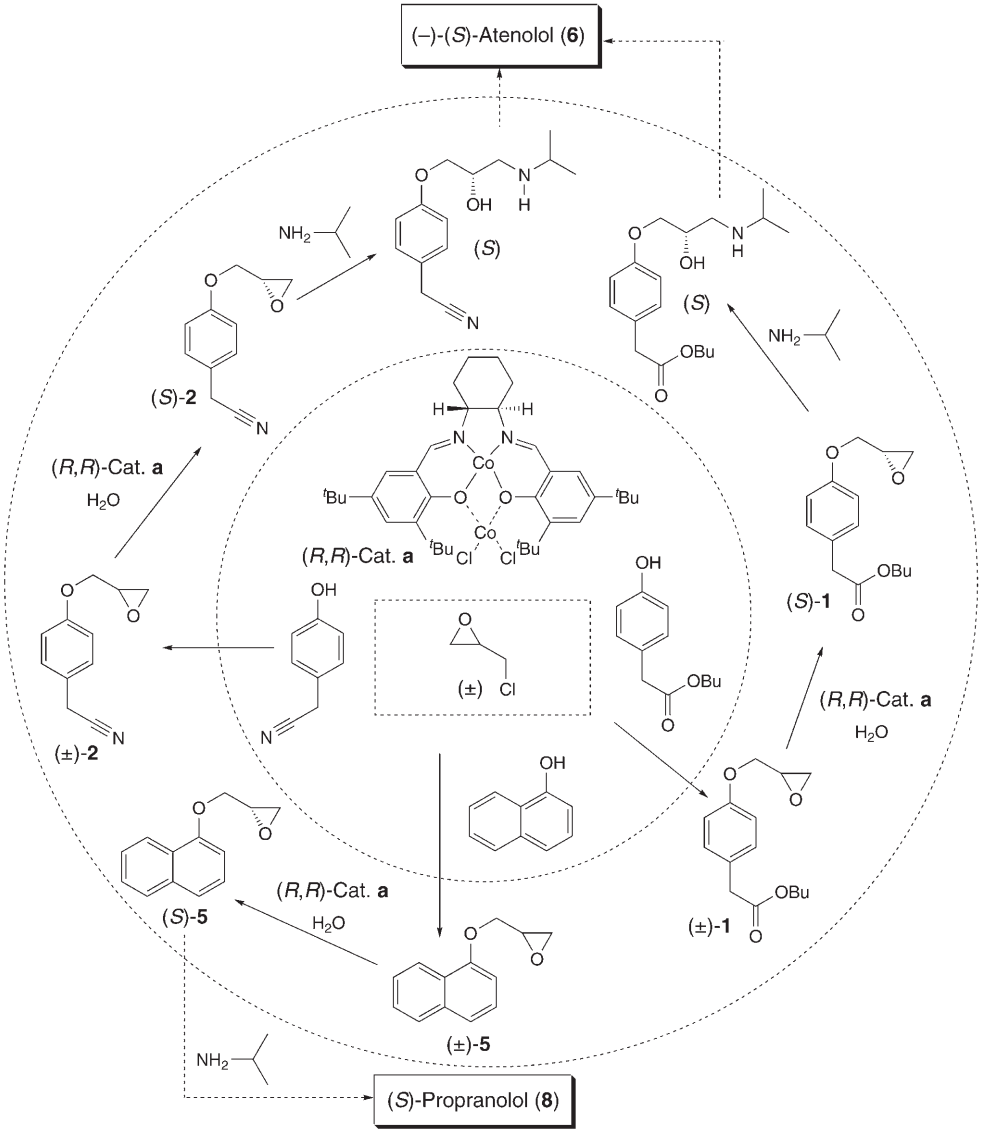

The bond lengths Co–O, Fe–O, and Ni–O of catalysts **a**, **b**, and **e** were 1.76, 1.85, and 1.82 Å, respectively, and the coordination numbers *ca.* 2, 1, and 2, respectively (*Table 5*). It is worth comparing these M–O distances with those of related complexes. The Co–O distance for Co–$CoCl_2$ complex **a** is slightly shorter than in the *Jacobsen*-type catalyst **A** [13], but similar to the O–Co atomic radii (R_{sum}) determined from

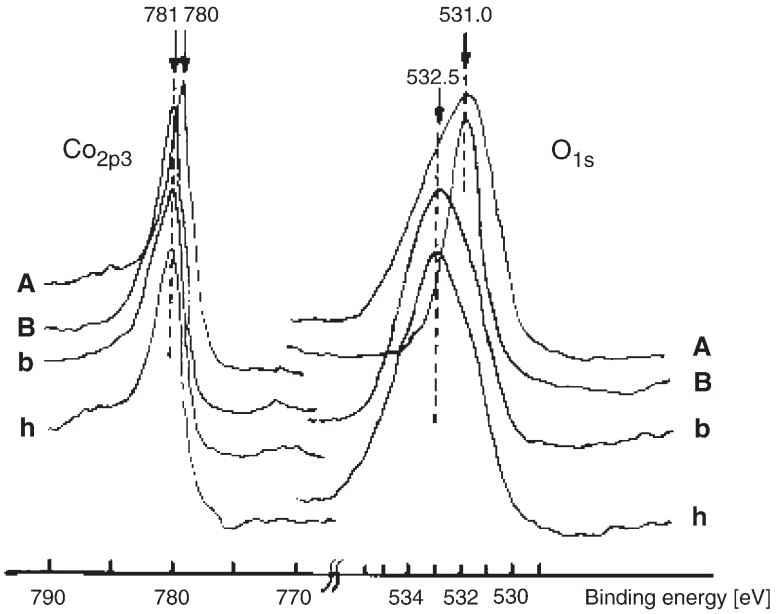

Fig. 4. *ESCA Spectra* (Co2p3 and O1s) *of* Jacobsen-*type catalyst* **A** *Co^{III}–OAc, [Co(Salen)]-type catalyst* **B**, *Co^{II}–$NiCl_2$ catalyst* **b**, *and Co^{II}–$Co(NO_3)_2$ catalyst* **h**

Table 4. *Characterization of Chiral [Co(salen)]-Type Complexes by Electron Spectroscopy for Chemical Analysis* (ESCA). Electron-binding energies in eV.

Catalyst	Catalyst type	Co2p3	O1s
A	Co^{III}–OAc (*Jacobsen*-type catalyst)	780.0	531.0
B	Co^{II}–(only salen-type ligand)	781.0	531.4
a	Co^{II}–$CoCl_2$	781.0	532.0
b	Co^{II}–$NiCl_2$	781.0	532.5
e	Co^{II}–$FeCl_3$	781.9	532.0
f	Co^{II}–$Zn(NO_3)_2$	781.0	532.6
g	Co^{II}–$Ni(NO_3)_2$	782.2	533.4
h	Co^{II}–$Co(NO_3)_2$	781.0	532.5

literature values [14]. Futhermore, the Ni–O and Fe–O bond lengths are about the same as the O–Ni and O–Fe atomic radii [14] and those of analogous complexes [15][16]. For all complexes, the M–O bond lengths showed a direct correlation to the atomic radii of the metal to the O-atom. Such bond lengths can be generated only by the attachment of transition metals to the O-atoms of the salen-type ligand, and it is suggested that the transition-metal cation attached to these O-atoms adopts a stable tetrahedral coordination polyhedron. The coordination polyhedron of the [Co^{II}(salen)]-type moiety presumably remains essentially a planar structure when it acts as ligand, but the transition-metal atom attached to the O-atoms of the salen-type ligand

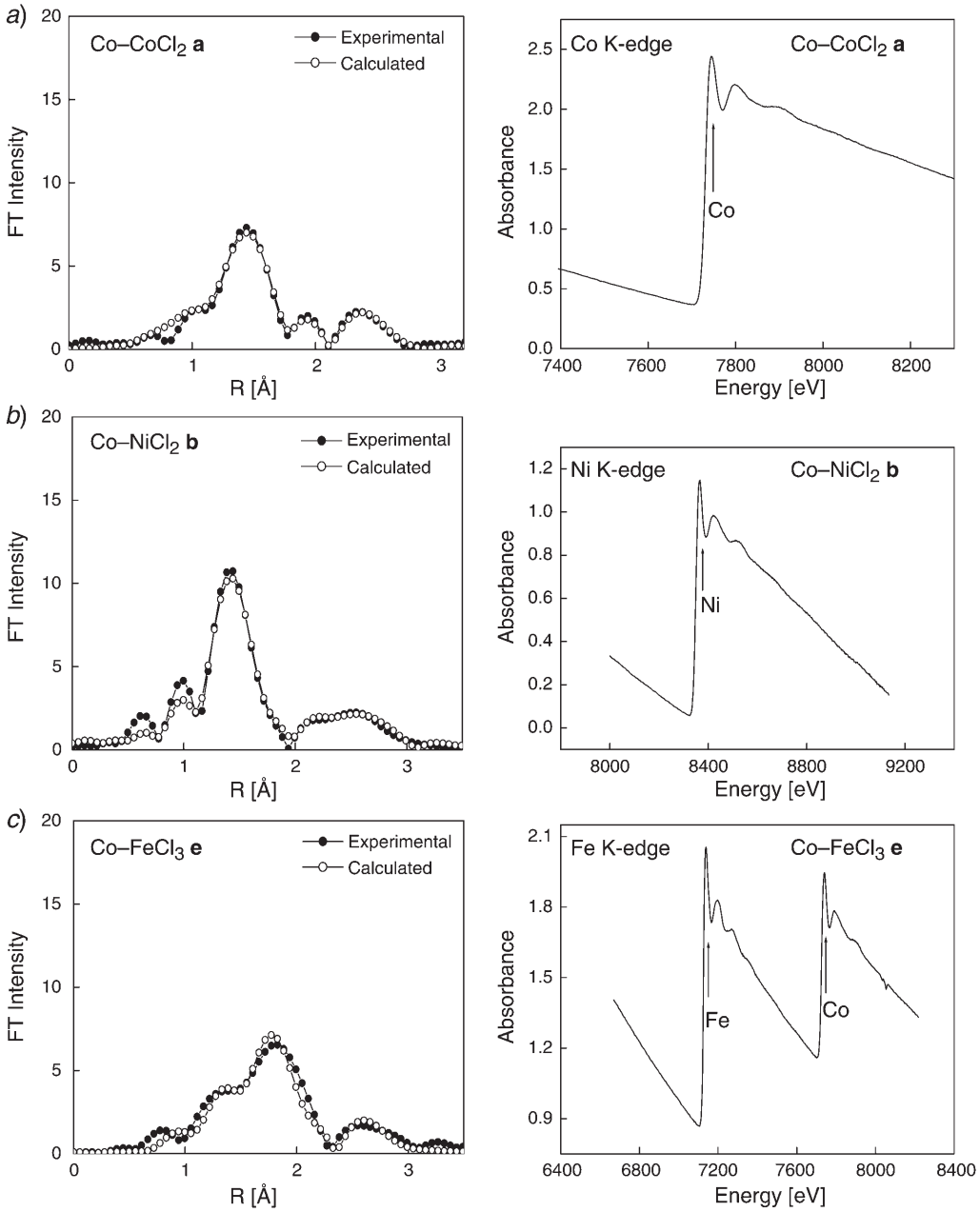

Fig. 5. *Comparison of the measured* (experimental) *and calculated curves by* Fourier-*transform curve fitting in the EXAFS analysis of [Co(Salen)]-type complexes* **a**, **b**, *and* **e**

Table 5. *EXFAS Results of Chiral [Co(salen)]-Type Complexes by Curve Fitting with the FEFF6 Program*

	Pair	R [Å][a])	*CN* [b])
Catalyst **a** (Co–$CoCl_2$)	Co–O	1.76	2.20
	Co–Cl	1.98	2.47
	Co–Co	2.46	1.38
Catalyst **b** (Co–$NiCl_2$)	Ni–O	1.82	2.02
	Ni–Cl	1.96	2.11
	Ni–Co	2.79	1.08
Catalyst **e** (Co–$FeCl_3$)	Fe–O	1.85	1.44
	Fe–Cl	2.20	3.10
	Fe–Co	2.98	1.01

[a]) Bond length. [b]) Coordination number.

does not need to lie exactly in the same plane as the central Co-atom with the four donor atoms. In addition, the Co–Cl, Fe–Cl, and Ni–Cl bond lengths of the coordinating transition-metal salts were calculated as 1.98, 2.20, and 1.96 Å for **a**, **e**, and **b**, respectively, thus, differing from the corresponding M–O bond lengths. The coordination numbers for the metal to chloride ion are *ca.* 2, 3, and 2, respectively, thus well matching those of the original salts such as $CoCl_2$, $FeCl_3$, and $NiCl_2$ used for the synthesis of **a**, **e**, and **b** respectively. The mol ratio of the Co-center in the salen-type structure to the transition-metal center was controlled as 1:1 for each case in the synthesis steps. That this ratio was conserved in the binuclear complex was confirmed by the EXAFS analysis. In addition, for the representative of Co–$CoCl_2$, Co–$NiCl_2$, and Co–$FeCl_3$ complexes **a**, **b**, and **e**, respectively, all the measured and calculated curves of the EXAFS analysis were perfectly matching (*Fig. 5*, *a–c*).

The FAB-MS of Co–$CoCl_2$ complex **a** and Co–$FeCl_3$ complex **e** provided a direct evidence of the configuration and formation of bimetallic complexes. Complexes **a** and **e** showed significant peaks for M^+ at *m*/*z* 734 and 762 together with a peak of the mononuclear complex **B** at *m*/*z* 603 and 599 (*Figs. 6* and *7*). These MS data of catalysts **a** and **e** showed that the bimetallic salen-type complexes are not physical mixtures of a [Co^{II}(salen)]-type complex and a transition-metal salt.

In conclusion, we explored new chiral [Co(salen)]-type complexes efficient as catalysts in HKR of terminal (±)-oxiranes. The new complexes produced a high enantioselectivity in each reaction, providing more than 98% ee and high product yields. We hope that these bimetallic complexes will catalyze other important asymmetric reactions in high yield and with excellent enantioselectivity. Efforts are underway to elucidate the mechanistic details and other significant applications of this catalytic system.

Experimental Part

General. (*R*,*R*)-*N*,*N*′-Bis[3,5-di-(*tert*-butyl)salicylidene]cyclohexane-1,2-diaminocobalt(II) (={{2,2′-{(1*R*,2*R*)-Cyclohexane-1,2-diylbis[(nitrilo-κ*N*)methylidyne]}bis[4,6-bis(1,1-dimethylethyl)phenolato-κ*O*](2–)}cobalt; **B**) was purchased from *Aldrich*. THF, CH_2Cl_2, and hexane were used after distillation.

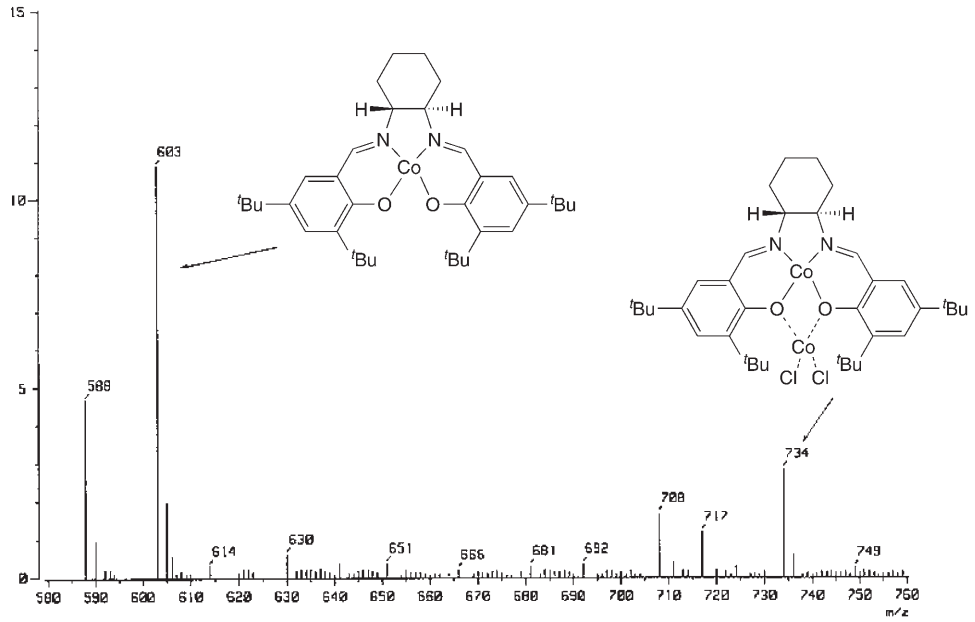

Fig. 6. *FAB-MS of Co^{II}–$CoCl_2$ catalyst* **a**

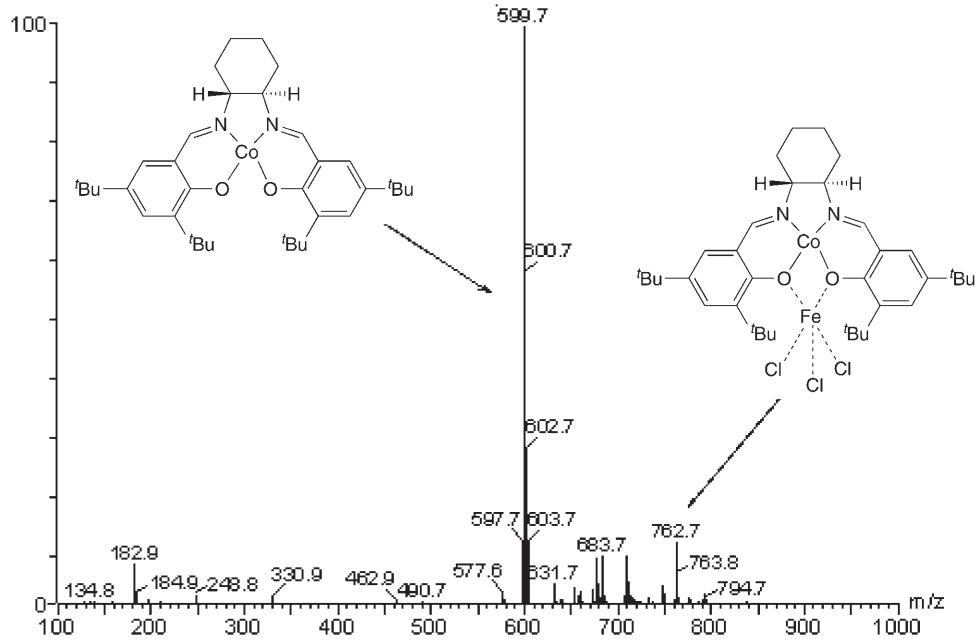

Fig. 7. *FAB-MS of Co^{II}–$FeCl_3$ catalyst* **e**

Transition-metal salts and all other reagents were purchased from *Aldrich*, *Fluka*, and *TCI*. Gas chromatography (GC): *Hewlett-Packard 5890-II* instrument, FID detector, chiral column *Chiraldex G-TA* and *A-TA* (20 m × 0.25 mm i.d.; *Astec*; *HP-3396* integrator with *HP* Chem-Station software for data analysis. Chiral HPLC: *Younglin* instrument, *Chiralcel®-OD* column (24 cm × 0.46 cm i.d.; *Chiral Technologies, Inc.*) and *(*R,R*)-Whelk-O1*/*(*S,S*)-Whelk-O1* column (24 cm × 0.46 cm i.d.; *Regis*) at 254 nm. IR Spectra: in cm^{-1}. ^{13}C-NMR Spectra: 400-MHz-FT-NMR spectrophotometer (*Varian Unity Nova-400*), at r.t.; δ in ppm, J in Hz. Fast-atom bombardment (FAB) MS: *Jeol JMS-AX505WA*/*HP 5890-II* spectrometer. EXAFS Analysis: *Rigaku* model *R-XAS* spectrometer (*Rigaku*, Japan), with Co K-edge energy (7708.9 eV), Ni K-edge energy (8332.8 eV), and Fe K-edge energy (7112.0 eV) radiation, data stimulated by the FEFF 6 program [12]. ESCA Data: *Sigma-Probe* (*Thermo VG*, U.K.) spectrometer, with MgK_α radiation as an excitation source ($h\nu = 1253.6$ eV); binding energy as compared with a reference of catalyst **B** or *Jacobsen*-type catalyst **A**.

Catalyst Preparation: General Procedure. The bimetallic chiral [Co(salen)]-type complexes were synthesized by mixing in a 1:1.2 mol ratio complex **B** and a transition-metal salt in THF. The mixture was stirred in an open flask for 2 h. After the evaporation of the solvent, the obtained catalyst was collected by dissolution in CH_2Cl_2 to remove the unreacted metal salts. Evaporation of CH_2Cl_2 gave a dark green or dark brown solid powder; yield 95–98%.

Hydrolytic Kinetic Resolution: General Procedure. In an oven-dried 25 ml flask equipped with a stirring bar, one of the (*R*,*R*) catalysts **a**–**h** (0.05–1.0 mol-%) and a terminal (±)-oxirane (40 mmol, 1.0 equiv.) were stirred at r.t. H_2O (22 mmol, 0.55 equiv.) was added dropwise (mild exothermic reaction). The mixture was stirred until an optically pure terminal oxirane was formed. The recovered oxirane was then filtered through a $MgSO_4$ pad. The optically pure product was isolated by bulb-to-bulb distillation (sealless tube oven *Eyela KRD100*, *Tokyo Rikakikai Co. Ltd.*) into a receiving flask at 0°. The ee of the chiral oxirane was determined by GC (chiral capillary column).

*Dichloro{μ-{{2,2′-{(1*R,2R*)-cyclohexane-1,2-diylbis[(nitrilo-κ*N*)methylidyne]}bis[4,6-bis(1,1-dimethylethyl)phenolato-κ*O*:κ*O*]}(2−)}}dicobalt* (**a**). IR (KBr): 2954, 2866, 1637, 1611, 1525, 1465, 1369, 1249, 1202, 1165, 1023, 925, 835, 782, 754, 636, 595. ^{1}H-NMR (400 MHz, (D_6)DMSO): 1.28 (*s*, 18 H); 1.50–1.62 (*m*, 2 H); 1.72 (*s*, 18 H); 1.80–1.95 (*m*, 4 H); 1.96–1.98 (*m*, 2 H); 3.1–3.2 (*m*, 2 H); 3.5–3.7 (*m*, 2 H); 7.40 (*d*, $J = 2.4$, 2 H); 7.45 (*d*, $J = 2.4$, 2 H); 7.78 (*s*, 2 H). ^{13}C-NMR (400 MHz, (D_6)DMSO): 25.8; 31.1; 32.2; 36.4; 67.6; 69.9; 119.2; 129.3; 136.4; 142.3; 162.5. FAB-MS: 734.0 ($C_{36}H_{52}Cl_2Co_2N_2O_2^+$; calc. 733). Anal. calc. for $C_{36}H_{52}Cl_2Co_2N_2O_2$ (732): C 58.94, H 7.14, Cl 9.67, Co 16.07, N 3.82, O 4.36; found: C 59.03, H 7.00, Cl 9.52, Co 16.00, N 3.79, O 4.45.

*{μ-{{2,2′-{(1*R,2R*)-Cyclohexane-1,2-diylbis[(nitrilo-κ*N*)methylidyne]}bis[4,6-bis(1,1-dimethylethyl)phenolato-κ*O*:κ*O*]}(2−)}}(dichloronickel)cobalt* (**b**). IR (KBr): 2952, 2866, 1616, 1523, 1449, 1436, 1361, 1388, 1253, 1203, 1172, 929, 867, 833, 783, 744, 640, 570, 543. ^{1}H-NMR (400 MHz, (D_6)DMSO): 1.28 (*s*, 18 H); 1.50–1.57 (*m*, 2 H); 1.72 (*s*, 18 H); 1.80–1.95 (*m*, 4 H); 1.96–1.98 (*m*, 2 H); 3.0–3.1 (*m*, 2 H); 3.5–3.6 (*m*, 2 H); 7.42 (*d*, $J = 2.4$, 2 H); 7.45 (*d*, $J = 2.4$, 2 H); 7.78 (*s*, 2 H). FAB-MS: 731.0 ($C_{36}H_{52}Cl_2CoN_2NiO_2^+$; calc. 732). Anal. calc. for $C_{36}H_{52}Cl_2CoN_2NiO_2$: C 58.96, H 7.15, Cl 9.67, Co 8.04, N 3.82, Ni 8.00, O 4.36; found: C 59.93, H 7.11, Cl 9.60, Co 8.00, N 3.80, Ni 8.00, O 4.35.

*{μ-{{2,2′-{(1*R,2R*)-Cyclohexane-1,2-diylbis[(nitrilo-κ*N*)methylidyne]}bis[4,6-bis(1,1-dimethylethyl)phenolato-κ*O*:κ*O*}(2−)}}(dichlorozinc)cobalt* (**c**). IR (KBr): 2950, 2866, 1604, 1523, 1461, 1388, 1361, 1249, 1203, 1033, 907, 866, 833, 788, 574. ^{1}H-NMR (400 MHz, (D_6)DMSO): 1.29 (*s*, 18 H); 1.50–1.58 (*m*, 2 H); 1.73 (*s*, 18 H); 1.80–1.95 (*m*, 4 H); 1.96–1.98 (*m*, 2 H); 3.0–3.1 (*m*, 2 H); 3.5–3.6 (*m*, 2 H); 7.42 (*d*, $J = 2.4$, 2 H); 7.45 (*d*, $J = 2.4$, 2 H); 7.79 (*s*, 2 H). ^{13}C-NMR (400 MHz, (D_6)DMSO): 24.2; 29.3; 30.3; 31.4; 33.5; 35.7; 66.9; 86.4; 118.4; 128.6; 141.6; 161.8; 164.4. Anal. calc. for $C_{36}H_{52}Cl_2CoN_2O_2Zn$ (740): C 58.43, H 7.08, Cl 9.58, Co7.96, N 3.79, O 4.32, Zn 8.84; found: C 58.40, H 7.00, Cl 9.49, Co7.95, N 3.67, O 4.35, Zn 8.79.

*Dichloro(cobalt){μ-{{2,2′-{(1*R,2R*)-cyclohexane-1,2-diylbis[(nitrilo-κ*N*)methylidyne]}bis[4,6-bis-(1,1-dimethylethyl)phenolato-κ*O*:κ*O*}(2−)}}iron* (**d**). IR (KBr): 2958, 2866, 1604, 1535, 1461, 1431, 1388, 1342, 1311, 1253, 1203, 1172, 1029, 907, 840, 783, 740, 640, 543. ^{1}H-NMR (400 MHz, (D_6)DMSO): 1.27 (*s*, 18 H); 1.50–1.58 (*m*, 2 H); 1.71 (*s*, 18 H); 1.80–1.95 (*m*, 4 H); 1.96–1.98 (*m*, 2 H); 3.0–3.1 (*m*, 2 H); 3.5–3.6 (*m*, 2 H); 7.42 (*d*, $J = 2.4$, 2 H); 7.45 (*d*, $J = 2.4$, 2 H); 7.79 (*s*, 2 H). Anal. calc. for

$C_{36}H_{52}Cl_2CoFeN_2O_2$ (730): C 59.19, H 7.17, Cl 9.71, Co 8.07, Fe 7.64, N 3.83, O 4.38; found: C 59.15, H 7.15, Cl 9.69, Co 8.00, Fe 7.62, N 3.79, O 4.36.

*Trichloro(cobalt){μ-{{2,2′-{(1*R,*2*R*)-cyclohexane-1,2-diylbis[(nitrilo-κ*N*)methylidyne]}bis[4,6-bis(1,1-dimethylethyl)phenolato-κ*O*:κ*O*]}(2−)}}iron* (**e**). IR (KBr): 2954, 2866, 1634, 1609, 1511, 1459, 1365, 1251, 1208, 1169, 1035, 985, 834, 785, 734, 640, 597. ^{1}H-NMR (400 MHz, (D_6)DMSO): 1.27 (*s*, 18 H); 1.55–1.68 (*m*, 2 H); 1.71 (*s*, 18 H); 1.86–1.95 (*m*, 4 H); 1.9–2.20 (*m*, 2 H); 3.0–3.2 (*m*, 2 H); 3.5–3.8 (*m*, 2 H); 7.41 (*d*, *J* = 2.4, 2 H); 7.59 (*d*, *J* = 2.4 2 H); 7.76 (*s*, 2 H). ^{13}C-NMR (400 MHz, (D_6)DMSO): 24.5; 25.8; 29.3; 30.9; 31.5; 35.7; 69.21; 119.3; 128.4; 134.1; 142.3; 158.5; 162.1; 164.8. FAB-MS: 762.7 ($C_{36}H_{52}Cl_3CoFeN_2O_2^+$; calc. 764). Anal. calc. for $C_{36}H_{52}Cl_3CoFeN_2O_2$ (764): C 56.90, H 7.10, Cl 13.62, Co 7.55, Fe 7.15, N 3.59, O 4.10; found: C 56.85, H 7.13, Cl 13.66, Co 7.60, Fe 7.20, N 3.62, O 4.09.

*{μ-{{2,2′-{(1*R,*2*R*)-cyclohexane-1,2-diylbis[(nitrilo-κ*N*)methylidyne]}bis[4,6-bis(1,1-dimethylethyl)phenolato-κ*O*:κ*O*]}(2−)}}[di(nitrato-κ*N*)zinc]cobalt* (**f**). IR (KBr): 2950, 2863, 1635, 1608, 1523, 1461, 1361, 1253, 1200, 1172, 1026, 926, 833, 783, 744, 640, 597. ^{1}H-NMR (400 MHz, (D_6)DMSO): 1.25 (*s*, 18 H); 1.54–1.64 (*m*, 2 H); 1.71 (*s*, 18 H); 1.80–1.90 (*m*, 4 H); 1.95–1.97 (*m*, 2 H); 3.1–3.2 (*m*, 2 H); 3.5–3.6 (*m*, 2 H); 7.40 (*d*, *J* = 2.4, 2 H); 7.42 (*d*, *J* = 2.4, 2 H); 7.74 (*s*, 2 H). ^{13}C-NMR (400 MHz, (D_6)DMSO): 24.3; 25.1; 29.5; 30.5; 31.5; 33.5; 67.0; 69.2; 118.5; 128.6; 129.0; 135.8; 141.7; 161.8; 164.4. FAB-MS: 791.8 ($C_{36}H_{52}CoN_4O_8Zn^+$; calc. 792). Anal. calc. for $C_{36}H_{52}CoN_4O_8Zn$ (793): C 54.52, H 6.61, Co 7.43, N 7.06, O 16.14, Zn 8.24; found: C 54.50, H 6.65, Co 7.39, N 7.10, O 16.20, Zn 8.20.

*{μ-{{2,2′-{(1*R,*2*R*)-Cyclohexane-1,2-diylbis[(nitrilo-κ*N*)methylidyne]}bis[4,6-bis(1,1-dimethylethyl)phenolato-κ*O*:κ*O*]}(2−)}}[di(nitrato-κ*N*)nickel]cobalt* (**g**). IR (KBr): 2950, 2866, 1616, 1527, 1434, 1384, 1253, 1203, 1172, 871, 833, 783, 574, 543. ^{1}H-NMR (400 MHz, (D_6)DMSO): 1.27 (*s*, 18 H); 1.54–1.58 (*m*, 2 H); 1.73 (*s*, 18 H); 1.80–1.85 (*m*, 4 H); 1.96–1.97 (*m*, 2 H); 3.0–3.1 (*m*, 2 H); 3.5–3.6 (*m*, 2 H); 7.41 (*d*, *J* = 2.4, 2 H); 7.43 (*d*, *J* = 2.4, 2 H); 7.77 (*s*, 2 H). Anal. calc. for $C_{36}H_{52}CoN_4NiO_8$ (786): C 54.98, H 6.66, Co 7.49, N 7.12, Ni 7.46, O 16.28; found: C 54.95, H 6.54, Co 7.45, N 7.09, Ni 7.45, O 16.25.

*{μ-2,2′-{(1*R,*2*R*)-Cyclohexane-1,2-diylbis[(nitrilo-κ*N*)methylidyne]}bis[4,6-bis(1,1-dimethylethyl)phenolato-κ*O*:κ*O*](2−)}}bis(nitrato-κ*N*)dicobalt* (**h**). IR (KBr): 2950, 2863, 1635, 1608, 1523, 1461, 1361, 1253, 1200, 1172, 1026, 926, 833, 783, 744, 640, 597. ^{1}H-NMR (400 MHz, (D_6)DMSO): 1.24 (*s*, 18 H); 1.55–1.68 (*m*, 2 H); 1.69 (*s*, 18 H); 1.86–1.95 (*m*, 2 H); 1.96–2.20 (*m*, 2 H); 3.0–3.2 (*m*, 2 H); 3.5–3.8 (*m*, 2 H); 7.40 (*d*, *J* = 2.4, 2 H); 7.59 (*d*, *J* = 2.4, 2 H); 7.74 (*s*, 2 H). ^{13}C-NMR (400 MHz, (D_6)DMSO): 24.3; 25.1; 29.5; 30.4; 31.5; 33.5; 35.7; 66.9; 69.2; 118.5; 128.6; 129.0; 135.8; 141.6; 161.8; 164.4. FAB-MS: 785.3 ($C_{36}H_{52}Co_2N_4O_8^+$; calc. 786.2). Anal. calc. for $C_{36}H_{52}Co_2N_4O_8$ (786): C 54.96, H 6.66, Co 14.98, N 7.12, O 16.27; found: C 54.55, H 6.67, Co 15.00, N 7.15, O 16.30.

*Butyl 4-{[(2*S*)-Oxiran-2-yl]methoxy}benzeneacetate* ((*S*)-**1**; *Table 2*, *Entry 8*). $[\alpha]_D^{29} = +2.9$ (*c* = 1, $CHCl_3$). ^{1}H-NMR (400 MHz, $CDCl_3$): 0.88 (*t*, *J* = 7.2, 3 H); 1.31 (*q*, *J* = 7.6, 2 H); 1.58 (*q*, *J* = 8, 2 H); 2.73–2.90 (*m*, 2 H); 3.10–3.20 (*m*, 1 H); 3.54 (*s*, 2 H); 3.93 (*q*, *J* = 5.2, 1 H); 4.09 (*t*, *J* = 6.8, 2 H); 4.17–4.21 (*m*, 2 H); 6.76 (*d*, *J* = 8.8, 2 H); 7.10 (*d*, *J* = 8.4, 2 H). ^{13}C-NMR (400 MHz, $CDCl_3$): 13.3; 18.7; 30.2; 40.0; 50.9; 64.2; 68.5; 114.3; 126.6; 129.9; 157.2; 173.1.

*Butyl 4-{(2*S*)-2-Hydroxy-3-[(1-methylethyl)amino]propoxy}benzeneacetate* (**5**). $[\alpha]_D^{29} = +36$ (*c* = 0.5, MeOH). IR (KBr): 3290, 3210, 1724. ^{1}H-NMR (400 MHz, $CDCl_3$): 0.96 (*t*, *J* = 7.6, 3 H); 1.08 (*d*, *J* = 6.4, 6 H); 1.31–1.60 (*m*, 4 H); 2.4 (*s*, 2 H); 2.79–2.86 (*m*, 3 H); 3.53 (*s*, 2 H); 3.96–4.09 (*m*, 5 H); 6.85 (*d*, *J* = 8.8, 2 H); 7.17 (*d*, *J* = 8.8, 2 H). ^{13}C-NMR (400 MHz, $CDCl_3$): 13.6; 19.0; 30.6; 48.9; 49.2; 64.6; 68.4; 70.5; 114.6; 126.6; 130.2; 157.7; 171.9.

*Methyl 4-{[(2*S*)-Oxiran-2-yl]methoxy}benzeneacetate* ((*S*)-**4**; *Table 2*, *Entry 17*). $[\alpha]_D^{29} = +10.5$ (*c* = 1, MeOH) ([4]: $[\alpha]_D^{21} = +5.7$ (*c* = 1, $CHCl_3$)). IR (neat): 3000, 2949, 1738. ^{1}H-NMR (400 MHz, $CDCl_3$): 2.71–2.73 (*m*, 1 H); 2.86–2.88 (*m*, 1 H); 3.30 −3.33 (*m*, 1 H); 3.55 (*s*, 2 H); 3.66 (*s*, 3 H); 3.89 (*q*, *J* = 8, 1 H); 4.18 (*dd*, *J* = 11.2, 2.8, 1 H); 6.85 (*d*, *J* = 8, 2 H); 7.15 (*d*, *J* = 8, 2 H). ^{13}C-NMR (400 MHz, $CDCl_3$): 40.1; 44.5; 50.0; 51.8; 68.6; 114.5; 126.4; 130; 157.3; 171.9.

*Ethyl 4-{[(2*S*)-Oxiran-2-yl]methoxy}benzeneacetate* ((*S*)-**3**; *Table 2*, *Entry 13*). $[\alpha]_D^{29} = +36.0$ (*c* = 1, MeOH). IR (neat): 2982, 2929, 1735. ^{1}H-NMR (400 MHz, $CDCl_3$): 1.25 (*t*, *J* = 1.2, 3 H); 2.70–2.80 (*m*, 1 H); 2.84–2.90 (*m*, 1 H); 3.30 (*q*, *J* = 6, 1 H); 3.54 (*s*, 2 H); 3.93 (*q*, *J* = 5.6, 1 H); 4.14 (*q*, *J* = 7, 2 H); 4.20 (*dd*, *J* = 12, 4.4, 1 H); 6.86 (*d*, *J* = 7.2, 2 H); 7.18 (*d*, *J* = 6.8, 2 H). ^{13}C-NMR (400 MHz, $CDCl_3$): 14.1; 40.3; 44.5; 50.0; 60.7; 68.6; 114.5; 126.5; 130.0; 157.2; 171.6.

4-{[(2S)-Oxiran-2-yl]methoxy}benzeneacetonitrile ((*S*)-**2**; *Table 2*, *Entry 4*). $[\alpha]_D^{30} = +8.0$ ($c = 1$, MeOH). IR (KBr): 2939, 2248, 1512, 1249. ^{1}H-NMR (400 MHz, $CDCl_3$): 2.71 (*dd*, $J = 3.6, 1.6, 1$ H); 2.87 (*t*, $J = 4.4$, 1 H); 3.31–3.32 (*m*, 1 H); 3.65 (*s*, 2 H); 3.92 (*dd*, $J = 5.6$, 1 H); 4.22 (*dd*, $J = 2.8, 2.4$, 1 H); 6.89 (*d*, $J = 8$, 2 H); 7.21 (*d*, $J = 8.4$, 2 H). ^{13}C-NMR (400 MHz, $CDCl_3$): 22.8; 44.6; 50.0; 68.8, 115.1; 118.0; 122.3; 129.0; 158.0.

4-{(2S)-2-Hydroxy-3-[(1-methylethyl)amino]propoxy}benzeneacetonitrile. $[\alpha]_D^{29} = +12.8$ ($c = 1$, MeOH). IR (KBr): 3305, 3055, 2958, 2912, 2835, 2252, 1512, 1245. ^{1}H-NMR (400 MHz, $CDCl_3$): 1.1 (*s*, 6 H); 2.7 (*m*, 1 H); 2.9 (*d*, $J = 12$, 2 H); 3.67 (*s*, 2 H); 3.9–4.2 (*m*, 3 H); 6.92 (*d*, $J = 8.8$, 2 H); 7.23 (*d*, $J =$ 8.4, 2 H). ^{13}C-NMR (400 MHz, $CDCl_3$): 22.8; 23.0; 23.1; 48.8; 49.2; 68.3; 68.9; 70.6; 115.0; 118.0; 121.9; 128.9; 129; 158.3.

4-{(2S)-2-Hydroxy-3-[(1-methylethyl)amino]propoxy}benzeneacetamide (*=(–)-(S)-Atenolol*; **6**). $[\alpha]_D^{230} = -16.5$ ($c = 1$, 1N HCl) ([4]: $[\alpha]_D^{29} = -17.0$ ($c = 1$, 1N HCl)). IR (KBr): 3352, 3174, 1639, 1242. ^{1}H-NMR (400 MHz, D_2O): 1.1 (*d*, $J = 2$, 6 H); 2.81–2.96 (*m*, 3 H); 3.58 (*s*, 2 H); 4.04–4.14 (*m*, 3 H); 7.04 (*d*, $J = 8.4$, 2 H); 7.30 (*d*, $J = 8.4$, 2 H). ^{13}C-NMR (400 MHz, D_2O): 20.95; 20.97; 41.0; 48.2; 48.6; 68.4; 70.6; 114.9; 115.2; 130.4; 130.6; 157.4; 178.0.

(2S)-1-[(-Methylethyl)amino]-3-(naphthalen-1-yloxy)propan-2-ol (*=(S)-Propranolol*; **8**) $[\alpha]_D^{29} = -29$ ($c = 1$, EtOH). IR (KBr): 3271, 2966, 2923, 2835, 1631, 1581, 1458, 1400, 1269, 1242, 1103, 1068, 914, 879, 790, 570. ^{1}H-NMR (400 MHz, $CDCl_3$): 1.1 (*d*, $J = 6.3$, 6 H); 2.8–2.9 (*m*, 1 H); 3.0 (*dd*, $J = 12.3$, 3.1, 1 H); 4.0–4.25 (*m*, 3 H); 6.83 (*d*, $J = 7$, 1 H); 7.37 (*t*, $J = 7.6$, 1 H); 7.40–7.50 (*m*, 3 H); 7.80 (*dd*, $J = 6.1$, 2.4, 1 H); 8.24 (*dd*, $J = 7.1, 3.0$, 1 H). ^{13}C-NMR (400 MHz, $CDCl_3$): 23.0; 23.2; 48.9; 49.4; 68.4; 70.6; 104.7; 120.4; 121.67; 125.0; 125.6; 126.2; 127.3; 134.3; 154.1.

REFERENCES

[1] N. Bodor, Y. Oshiro, T. Loftsson, M. Katovich, W. Caldwell, *Pharma. Res.* **1984**, 120; N. Bodor, A. A. El-Koussi, M. Kano, M. M. Khalifa, *J. Med. Chem.* **1988**, *31*, 1651.

[2] P. W. Erhardt, C. M. Woo, R. J. Gorczynski, W. G. Anderson, *J. Med. Chem.* **1982**, *25*, 1402.

[3] H. Mikuldas, I. Cepanec, A. Sporec, M. Litvic, V. Vinkovic, *J. Sep. Sci.* **2005**, *28*, 251.

[4] H. S. Bevinakatti, A. A. Banerji, *J. Org. Chem*. **1992**, *57*, 6003; H. S. Bevinakatti, A. A. Banerji, *J. Org. Chem*. **1991**, *56*, 5372; D. S. Bose, A. V. Narsaiah, *Bioorg. Med. Chem*. **2005**, *13*, 627; J. Akisanya, A. W. Parkins, J. W. Steed, *Org. Process Res. Dev*. **1998**, *2*, 274; J. F. Lorrow, S. E. Schaus, E. N. Jacobsen, *J. Am. Chem. Soc.* **1996**, *118*, 7420; D. A. Annis, E. N. Jacobsen, *J. Am. Chem. Soc.* **1999**, *121*, 4147.

[5] K. Kitaori, Y. Takehira, Y. Furukawa, H. Yamamoto, J. Otera, *J. Chem. Pharm. Bull*. **1997**, *45*, 412.

[6] S. E. Schaus, B. D. Brandes, J. F. Larrow, M. Tokunaga, K. B. Hansen, A. E. Gould, M. E. Furrow, E. N. Jacobsen, *J. Am. Chem. Soc*. **2002**, *124*, 1307; M. Tokunaga, J. F. Larrow, F. Kakiuchi, E. N. Jacobsen, *Science* (Washington, D. C.) **1997**, *277*, 936.

[7] C. K. Shin, S.-J. Kim, G.-J. Kim, *Tetrahedron Lett*. **2004**, *45*, 7429; S. S. Thakur, W. Li, S.-J. Kim, G.-J. Kim, *Tetrahedron Lett*. **2005**, *46*, 2263; S. S. Thakur, S.-W. Chen, W. Li, C. K. Shin, Y. M. Koo, G.-J. Kim, *Synth. Commun*. **2006**, *36*, 2371; S. S. Thakur, S.-W. Chen, W. Li, C. K. Shin, S.-J. Kim, Y. M. Koo, G.-J. Kim, *J. Organomet. Chem.* **2006**, *691*, 1862.

[8] R. G. Konsler, E. N. Jacobsen, *J. Am. Chem. Soc*. **1998**, *120*, 10780; R. Breinbauer, E. N. Jacobsen, *Angew. Chem., Int. Ed*. **2000**, *39*, 3604.

[9] T. Mathew, N. R.Shiju, K. Sreekumar, B. S. Rao, C. S. Gopinath, *J. Catal.* **2002**, *210*, 405.

[10] X. G. Luo, X. H Chen, X. Liu, R. T. Wang, Y. M. Xiong, G. Y. Wang, X. G. Qui, *Phys. Rev. B.* **2004**, *70*, 054520.

[11] A. Martínez, C. López, F. Márquez, I. Díaz, *J. Catal*. **2003**, *220*, 486.

[12] S. I. Zabinasky, J. J. Rehr, A. Ankudinov, R. C. Albers, E. J. Eller, *Phys. Rev. B* **1995**, *52*, 2995.

[13] J. M. Ready, E. N. Jacobsen, *J. Am. Chem. Soc.* **1999**, *121*, 6086.

[14] C. H. Suresh, N. Koga, *J. Phys. Chem., A* **2001**, *105*, 5940.

[15] L. Banci, C. Benelli, D. Gatteschi, *Inorg. Chem*. **1981**, *20*, 4397.

[16] C. J. O'Connor, D. P. Freyberg, E. Sinn, *Inorg. Chem.* **1979**, *18*, 1077.

Received June 18, 2007